

A TIME-DOMAIN GENERALIZED WIENER FILTER FOR MULTI-CHANNEL SPEECH SEPARATION

Yi Luo

Tencent AI Lab, Shenzhen, China

ABSTRACT

Frequency-domain neural beamformers are the mainstream methods for recent multi-channel speech separation models. Despite their well-defined behaviors and the effectiveness, such frequency-domain beamformers still have the limitations of a bounded oracle performance and the difficulties of designing proper networks for the complex-valued operations. In this paper, we propose a time-domain generalized Wiener filter (TD-GWF), an extension to the conventional frequency-domain beamformers that has higher oracle performance and only involves real-valued operations. We also provide discussions on how TD-GWF can be connected to conventional frequency-domain beamformers. Experiment results show that a significant performance improvement can be achieved by replacing frequency-domain beamformers by the TD-GWF in the recently proposed sequential neural beamforming pipelines.

Index Terms: Speech separation, Wiener filter, Neural network

1. INTRODUCTION

Recent studies on neural beamformers have significantly advanced the state-of-the-art of multi-channel speech enhancement and separation systems [1–3]. A neural beamformer typically first applies a neural network to extract the target sources in the noisy observations and then uses a conventional beamformer to perform spatial filtering. Despite a few studies that explored the effect of time-domain beamformers [4], frequency-domain beamformers such as the multi-channel Wiener filter (MCWF) and the minimum-variance distortionless response (MVDR) beamformers are the default choices since both the microphone array and target source characteristics can be estimated in the frequency domain in a much easier way [5].

Prior works on time-domain single-channel speech separation have discussed the potential drawbacks for conventional time-frequency (T-F) masking [6]. Similarly, there are also two core limitations of the conventional frequency-domain neural beamformers: the *upper-bound performance* and the *complex-valued operations*. On the one hand, the performance of neural beamformers are upper-bounded by their performance when the oracle target sources are used for the calculation of source-specific features such as the spatial covariance matrices, and the neural beamformers can fail when the upper-bound performance of the selected beamformer is bad. On the other hand, with more and more recent works started to apply neural networks on complex-valued spectrograms, how to properly handle the real and imaginary parts of the features in the nonlinear transforms becomes an important problem. Although a common way is to concatenate the real and imaginary parts into a larger feature to jointly model them [7–10], there are also methods that use different modules for real and imaginary parts and mimic the behavior of complex-valued operations [11–13]. Nevertheless, how to effectively incorporate nonlinear complex-valued operations to the neural beamformers is still a topic to discuss.

In this paper, we propose a simple time-domain generalized Wiener filter (TD-GWF) as an alternative to frequency-domain conventional beamformers for multi-channel speech separation. TD-GWF directly performs minimum mean-square error (MMSE) estimation on the full waveforms without the need for a signal transformation such as short-time Fourier transform (STFT). As a result, all operations in TD-GWF are real-valued and any existing neural network blocks can be easily used together with it. Moreover, TD-GWF introduces more degrees of freedom in the optimization problem to be solved and significantly improves the oracle performance with respect to common signal quality metrics. With certain hyperparameter configurations, we also show that conventional beamformers are special cases of the TD-GWF. For neural beamformers, we apply TD-GWF in the recently proposed *sequential neural beamforming* pipeline, where multiple iterations of separation and beamforming operations are utilized to gradually improve the overall performance [14–16]. Experiment results show that the oracle performance of TD-GWF is significantly higher than that of frequency-domain MCWF, and replacing the frequency-domain MCWF by TD-GWF in the sequential neural beamforming pipeline drastically improves the separation performance.

The rest of the paper is organized as follows. Section 2 briefly overviews the conventional filter-and-sum beamformers and introduces the proposed TD-GWF. Section 3 provides the experiment configurations. Section 4 presents the experiment results. Section 5 concludes the paper.

2. TIME-DOMAIN GENERALIZED WIENER FILTER

2.1. Conventional Filter-and-sum Beamformers

Given M channels of L -sample noisy observations $\{y_m\}_{m=1}^M, y_m \in \mathbb{R}^{1 \times L}$ and a source-of-interest (SOI) $x \in \mathbb{R}^{1 \times L}$, a standard filter-and-sum beamformer estimates M beamformer coefficients $\{h_m\}_{m=1}^M, h_m \in \mathbb{R}^{1 \times K}$ which are applied to $\{y_m\}_{m=1}^M$:

$$\hat{x} = \sum_{m=1}^M y_m \circledast h_m \quad (1)$$

where \circledast denotes the convolution operation, K denotes the length of the beamformer coefficients, and $\hat{x} \in \mathbb{R}^{1 \times L}$ is the estimated SOI.

Such beamforming process is typically done in the frequency domain:

$$\hat{x}(f) = \sum_{m=1}^M \mathbf{y}_m(f) \mathbf{h}_m(f) = \mathbf{h}(f)^H \mathbf{Y}(f) \quad (2)$$

where $\hat{x}(f), \mathbf{y}_m(f) \in \mathbb{C}^{1 \times T}$ denotes the f -th frequency component in the spectrogram of \hat{x}, \mathbf{y}_m , respectively, T denotes the number of frames in the spectrograms, $\mathbf{h}_m(f) \in \mathbb{C}$ denotes the beamformer

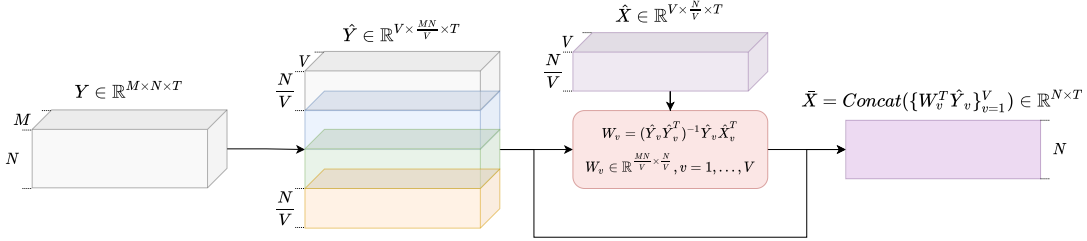


Fig. 1. Flowchart of the proposed time-domain generalized Wiener filter (TD-GWF).

coefficient for the m -th channel at the f -th frequency component, $\mathbf{Y}(f) \in \mathbb{C}^{M \times T}$ and $\mathbf{h}(f) \in \mathbb{C}^{M \times 1}$ represent the concatenation of the f -th frequency components and beamformer coefficients across all M channels, respectively, and $(\cdot)^H$ stands for the conjugate transpose.

The estimation of $\mathbf{h}(f)$ can be done by solving certain optimization problems designed for various purposes. For example, the frequency-domain MCWF (FD-MCWF) is defined for the MMSE estimation between the beamformed output and the estimated SOI, and its closed-form solution is:

$$\mathbf{h}_{\text{MCWF}}(f) = (\mathbf{Y}(f) \mathbf{Y}(f)^H)^{-1} \mathbf{Y}(f) \mathbf{x}(f)^H \quad (3)$$

2.2. Time-domain Generalized Wiener Filter

Figure 1 shows the procedure of the proposed TD-GWF. Note that similar to the use of spectrograms in conventional frequency-domain beamformers, we generate sequential features \mathbf{Y} and \mathbf{X} typically by applying a real-valued linear transform to the windowed waveforms similar to the one used in recent time-domain separation systems [6]:

$$\mathbf{Y}_{m,t} = \mathbf{y}_{m,t} \mathbf{B} \quad (4)$$

where $\mathbf{y}_{m,t} \in \mathbb{R}^{1 \times P}$ denotes the t -th frame of the windowed waveform with P sample points at the m -th channel, $\mathbf{B} \in \mathbb{R}^{P \times N}$ is the linear transformation matrix, or the real-valued waveform encoder, that can be either pre-defined or jointly optimized with the entire system, and $\mathbf{Y} \in \mathbb{R}^{M \times N \times T}$ is the N -dimension sequential features of the noisy observations.

The proposed time-domain generalized Wiener filter (TD-GWF) can be viewed as a generalized extension to the conventional beamformers. We first split each N -dimension sequential feature of \mathbf{Y} into V non-overlapped groups of $\frac{N}{V}$ -dimension sub-features. The M channels of sub-features in the same group are then concatenated to form V groups of transformed features $\hat{\mathbf{Y}} \in \mathbb{R}^{V \times \frac{M \times N}{V} \times T}$. With the sequential feature of the estimated SOI $\mathbf{X} \in \mathbb{R}^{N \times T}$, we split it into V groups likewise to obtain the transformed feature $\hat{\mathbf{X}} \in \mathbb{R}^{V \times \frac{N}{V} \times T}$. Each group in $\hat{\mathbf{Y}}$ and $\hat{\mathbf{X}}$, denoted by $\hat{\mathbf{Y}}_v \in \mathbb{R}^{\frac{M \times N}{V} \times T}$ and $\hat{\mathbf{X}}_v \in \mathbb{R}^{\frac{N}{V} \times T}$, respectively, are used to calculate a Wiener filter $\mathbf{W}_v \in \mathbb{R}^{\frac{M \times N}{V} \times \frac{N}{V}}$:

$$\mathbf{W}_v = (\hat{\mathbf{Y}}_v \hat{\mathbf{Y}}_v^T)^{-1} \hat{\mathbf{Y}}_v \hat{\mathbf{X}}_v^T, v = 1, \dots, V \quad (5)$$

\mathbf{W}_v is then applied to $\hat{\mathbf{Y}}_v$ to obtain the v -th group of the output signal:

$$\bar{\mathbf{X}}_v = \mathbf{W}_v^T \hat{\mathbf{Y}}_v \quad (6)$$

The final output $\bar{\mathbf{X}} \in \mathbb{R}^{N \times T}$ is obtained by concatenating the V groups of outputs $\{\bar{\mathbf{X}}_v\}_{v=1}^V$ across the feature dimension:

$$\bar{\mathbf{X}} = \text{Concat}(\{\bar{\mathbf{X}}_v\}_{v=1}^V) \quad (7)$$

2.3. TD-GWF in the Sequential Neural Beamforming Pipeline

A general design of the sequential neural beamforming pipeline contains a *pre-separation* module, a *beamformer*, and a *post-enhancement* module. The pre-separation module first performs separation on the noisy observations to obtain a coarse estimation of the SOIs, and then the beamformer uses those estimations to calculate the beamformer coefficients. The beamformed outputs, typically together with the coarse estimations from the pre-separation module, are then sent to a post-enhancement module for further refinements. Such beamforming-refinement procedure can be repeated for multiple iterations to form a sequential neural beamforming pipeline. Current pipelines have investigated the use of FD-MCWF and FD-MVDR beamformers in the pipeline and reported significant performance improvements compared to separator-only or single-stage neural beamforming baselines.

The application of TD-GWF in the existing sequential neural beamforming pipeline is straightforward. Figure 2 shows the pipeline of TD-GWF-based sequential neural beamformer. We follow the general design of [14] and [17] on the use of a single-channel separation network for both the pre-separation and the post-separation modules to save the computational cost, and we replace the FD-MCWF by the proposed TD-GWF. Moreover, we adopt the pipeline in [15] where each beamforming-refinement procedure is treated as one iteration, and the post-separation module receives the concatenation of the noisy observation at the reference channel, the separation outputs at previous iteration (the pre-separation outputs for the first iteration), and the TD-GWF outputs at the current iteration as inputs. The network parameters for the post-separation module is shared across all iterations. The training of the entire system is done by calculating the training objective on all outputs of the separation modules:

$$\mathcal{L}_{\text{obj}} = \frac{1}{K} \sum_{k=1}^K D_{\Pi}(\{\hat{\mathbf{X}}_c^{(k)}\}_{c=1}^C, \{\mathbf{X}_c\}_{c=1}^C) \quad (8)$$

where C denotes the total number of SOIs, K denotes the number of beamforming-refinement iterations, $D(\cdot)$ is a selected loss function, and $D_{\Pi}(\cdot)$ denotes the application of permutation invariant training (PIT) [18].

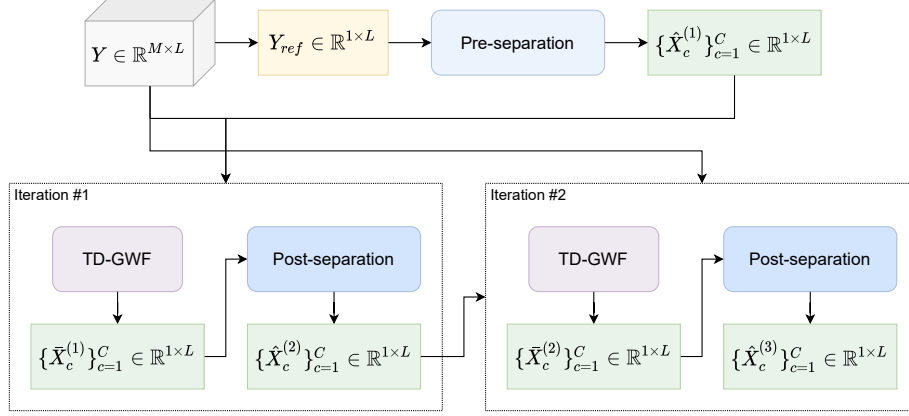


Fig. 2. Flowchart for the sequential neural beamforming pipeline.

2.4. Discussions

2.4.1. Relationship with Conventional Frequency-domain Beamformers

TD-GWF can be related to the conventional frequency-domain beamformers in two ways. On the one hand, it follows the general problem formulation of conventional beamformers where an optimization problem is defined on an estimated SOI to solve the beamformer coefficients. This can be easily observed since equation 3 and 5 only have differences on the dimension of the features and whether the operations are done in time-domain or frequency-domain. On the other hand, when the number of groups V equals to the feature dimension N , the TD-GWF coefficients are calculated on each feature dimension independently, and the shape of the coefficients becomes $M \times 1$. If we do not use the real-valued waveform encoder \mathbf{B} but use the Fourier transform to extract the sequential features, TD-GWF with $V = N$ falls back to the FD-MCWF in equation 3.

2.4.2. The Effect of Group Size

The group size V not only connects to the conventional beamformers when $V = N$, but also controls the overall model complexity. The concatenation of $\{\bar{X}_v\}_{v=1}^V$ across groups can be rewritten as the multiplication of two block-diagonal matrices:

$$\bar{\mathbf{X}} = \begin{bmatrix} \mathbf{W}_1^T & \dots & \mathbf{0} \\ \vdots & \ddots & \vdots \\ \mathbf{0} & \dots & \mathbf{W}_V^T \end{bmatrix} \begin{bmatrix} \hat{\mathbf{Y}}_1 & \dots & \mathbf{0} \\ \vdots & \ddots & \vdots \\ \mathbf{0} & \dots & \hat{\mathbf{Y}}_V \end{bmatrix} \quad (9)$$

For $V = 1$, $\mathbf{W}_v \in \mathbb{R}^{MN \times N}$ has no off-diagonal zero blocks and requires the most amount of float-point operations. A larger V increases the number of off-diagonal zero blocks and saves the computational cost, while at the cost of a fewer degrees of freedom. For $V = N$, the coefficient matrix becomes a diagonal matrix and is equivalent to the Hardamard product between the features of the noisy observations and the coefficients, which again falls back to the standard formulation of frequency-domain filtering.

Method	Window size	Group	SDR (dB)	SI-SDR (dB)
Mixture	—	—	-0.4	-0.5
FD-MCWF	32 ms	—	3.0	0.2
	64 ms		5.2	3.5
	128 ms		8.3	7.4
	256 ms		12.1	11.7
	512 ms		15.4	15.2
TD-GWF	2 ms	1	7.2	6.1
		2	5.3	4.2
		4	3.4	2.5
	4 ms	1	9.7	8.7
		2	7.1	6.1
		4	4.7	3.8
	8 ms	1	13.7	13.1
		2	9.8	9.1
		4	6.5	5.7
	16 ms	1	30.8	30.8
		2	16.6	16.4
		4	10.2	9.7

Table 1. Oracle performance of frequency-domain MCWF and the proposed TD-GWF. Oracle clean reverberant SOIs are used for the calculation of the beamformer coefficients.

3. EXPERIMENT CONFIGURATIONS

3.1. Dataset

We evaluate the proposed TD-GWF on a simulated noisy reverberant two-speaker dataset. 20000, 5000 and 3000 4-second long utterances are simulated at 16k Hz for training, validation and test sets, respectively. For each utterance, two speech signals and one noise signal are randomly selected from the 100-hour LibriSpeech subset [19] and the 100 Non-speech Corpus [20], respectively. The overlap ratio between the two speakers is uniformly sampled between 0% and 100%, and the two speech signals are shifted accordingly and rescaled to a random relative signal-to-noise-ratio (SNR) between 0 and 5 dB. The relative SNR between the speech mixture and the noise is randomly sampled between 10 and 20 dB. The transformed signals are then convolved with the room impulse response filters simulated by the image method [21] using the gpuRIR toolbox [22]. We refer the interested readers to [23] for a more detailed description on the room configurations. In this paper we only use the fixed geometry array dataset, in which a circular array with 6 evenly-distributed microphones with 10 cm diameter is randomly placed. The average distance between the SOIs and the array center is 2.9 ± 1.6 meters.

Model	# of param.	# of iter.	Speaker angle				Overlap ratio				Average
			<15°	15-45°	45-90°	>90°	<25%	25-50%	50-75%	>75%	
DPRNN-TasNet-S	1.3M	–	7.8	8.1	8.5	8.7	13.2	9.4	6.7	3.9	8.3
DPRNN-TasNet-L			8.2	8.5	8.8	9.0	13.4	9.7	7.0	4.4	8.6
FD-MCWF-TasNet (32 ms)	2.6M	1	8.9	9.3	9.9	10.2	14.3	10.8	8.0	5.2	9.6
FD-MCWF-TasNet (512 ms)		2	9.3	9.9	10.4	10.8	14.8	11.2	8.5	5.9	10.1
TD-GWF-TasNet (2 ms)	2.6M	1	10.1	10.3	10.5	11.0	15.4	11.8	8.8	6.0	10.5
TD-GWF-TasNet (4 ms)		2	11.4	11.9	12.0	12.5	16.5	13.2	10.6	7.4	11.9
TD-GWF-TasNet (8 ms)	2.6M	1	9.8	10.9	12.0	12.8	15.4	12.5	10.1	7.4	11.3
TD-GWF-TasNet (16 ms)		2	10.2	11.5	12.8	13.5	15.8	13.0	10.7	8.6	12.0
TD-GWF-TasNet (32 ms)	2.6M	1	10.0	11.1	11.9	12.6	15.6	12.6	10.1	7.3	11.4
TD-GWF-TasNet (512 ms)		2	10.7	11.9	12.9	13.6	16.3	13.3	11.0	8.5	12.3
TD-GWF-TasNet (1024 ms)	2.6M	1	10.1	10.9	11.5	12.0	15.5	12.3	9.5	7.2	11.1
TD-GWF-TasNet (2048 ms)		2	10.8	11.8	12.4	13.1	16.0	13.2	10.7	8.2	12.1

Table 2. Comparison of different models on the simulated 6-mic circular array. SI-SDR is reported on decibel scale.

3.2. Model configurations

We use the single-channel DPRNN-TasNet model [24] for the pre-separation and post-separation modules in the sequential neural beamforming pipeline where each module contains 3 DPRNN blocks. The window size and hop size in the TasNet’s waveform encoder and decoder are set to 2 ms (32 samples) and 1 ms (16 samples), respectively, and the number of filters in the encoder and decoder is set to 64. The input size and hidden size of the LSTM layers in the DPRNN blocks are set to 64 and 128, respectively. The separation is done by estimating a set of multiplicative masks applied to the TasNet’s encoder outputs, and we use a ReLU activation on the mask estimation layer to generate nonnegative masks.

For the TD-GWF module, we set the waveform encoder \mathbf{B} to identity matrix \mathbf{I} , which means that we only window the waveforms without applying a waveform encoder (note that \mathbf{B} is different from the TasNet’s encoder). The window size P for TD-GWF is set to 2 ms, 4 ms, 8 ms, and 16 ms for performance comparison, and the hop size is set to 25% of the window size P according to the common configurations in frequency-domain beamformers. The feature dimension N equals to the window size P .

3.3. Training and Evaluation

All models are trained for 100 epochs with the Adam optimizer [25] with an initial learning rate of 0.001. Signal-to-noise ratio (SNR) is used as the training objective $D(\cdot)$, and the clean reverberant SOIs are used as the training targets. The learning rate is decayed by 0.98 for every two epochs. Gradient clipping by a maximum gradient norm of 5 is applied, and the gradients are blocked between different beamforming-refinement iterations. We report the signal-to-distortion ratio (SDR) [26] and the scale-invariant signal-to-distortion ratio (SI-SDR) [27] for signal quality evaluation.

4. RESULTS AND DISCUSSIONS

4.1. Oracle Performance Comparison

We first compare the oracle performance of FD-MCWF and the proposed TD-GWF. Table 1 compares the two methods under various hyperparameter configurations. We can observe that the oracle performance of FD-MCWF is low when the window size is small, while the proposed TD-GWF achieves better oracle performance than a 256 ms window size FD-MCWF with only a 8 ms window size (with $\mathbf{W}_v \in \mathbb{R}^{\frac{768}{V} \times \frac{128}{V}}$). Moreover, the FD-MCWF with a 32 ms window size, which is often used as a default configuration in frequency-domain beamformers, has a lower oracle performance than TD-GWF with a 2 ms window size (with $\mathbf{W}_v \in \mathbb{R}^{\frac{192}{V} \times \frac{32}{V}}$). This shows

that TD-GWF has a much higher upper-bound performance than FD-MCWF without strict requirements on the frequency-domain resolution. As discussed in Section 2.4.2, a larger V corresponds to a lower oracle performance due to the decrease in the degrees of freedom, hence for the comparison of sequential neural beamforming pipelines we set the group size V to 1 and leave the effect of different V as future work.

4.2. Sequential Neural Beamforming with Different Numbers of Iterations

Table 2 presents the separation performance of various sequential neural beamforming pipelines. The first two rows provide the separation results of the single-channel-only baselines, where “-S” and “-L” denote “small” and “large” models with 3 and 6 DPRNN blocks, respectively. The rest of the table contains the results for the sequential neural beamforming pipelines with either FD-MCWF or TD-GWF for the beamforming stage. We can see that the FD-MCWF with 32 ms window is significantly worse than the TD-GWF with only 2 ms window in both 1 and 2 iteration configurations. While the FD-MCWF with 512 ms window can have better separation performance than the TD-GWF when speaker angle or the overlap ratio is small, the size of the spatial covariance matrix is too large ($\mathbb{C}^{4097 \times 4097}$) so that the computational cost is much higher than that of TD-GWF (with $\mathbf{W}_v \in \mathbb{R}^{384 \times 64}$ for 4 ms window). We also notice that the performance of TD-GWF with 8 ms window is slightly worse than that with 2 ms and 4 ms windows, and a possible reason for it is that the 8 ms window configuration leads to a large filter coefficient matrix $\mathbf{W}_v \in \mathbb{R}^{768 \times 128}$, which contains even more entries than the 4-second long utterances with 64000 samples. We suspect that large window sizes might be more useful and important for longer utterances, and we leave the validation of it as future work with a more diverse and realistic dataset.

5. CONCLUSION

We proposed the time-domain generalized Wiener filter (TD-GWF) as an alternative to conventional frequency-domain beamformers for multi-channel speech separation. TD-GWF has the advantage of a higher oracle performance and only contains real-valued operations, which makes it possible to apply any existing neural networks to any part of the filtering process. Experiment results on the sequential neural beamforming pipeline showed its effectiveness. Future works include the investigation of different group sizes, the use of different separator modules in the sequential neural beamforming pipeline, and the extension of TD-GWF to other forms of beamformers.

6. REFERENCES

- [1] T. Ochiai, S. Watanabe, T. Hori, J. R. Hershey, and X. Xiao, “Unified architecture for multichannel end-to-end speech recognition with neural beamforming,” *IEEE Journal of Selected Topics in Signal Processing*, vol. 11, no. 8, pp. 1274–1288, 2017.
- [2] X. Zhang, Z.-Q. Wang, and D. Wang, “A speech enhancement algorithm by iterating single-and multi-microphone processing and its application to robust ASR,” in *Acoustics, Speech and Signal Processing (ICASSP), 2017 IEEE International Conference on*. IEEE, 2017, pp. 276–280.
- [3] J. Heymann, M. Bacchiani, and T. N. Sainath, “Performance of mask based statistical beamforming in a smart home scenario,” in *Acoustics, Speech and Signal Processing (ICASSP), 2018 IEEE International Conference on*. IEEE, 2018, pp. 6722–6726.
- [4] K. Qian, Y. Zhang, S. Chang, X. Yang, D. Florencio, and M. Hasegawa-Johnson, “Deep learning based speech beamforming,” in *Acoustics, Speech and Signal Processing (ICASSP), 2018 IEEE International Conference on*. IEEE, 2018, pp. 5389–5393.
- [5] S. Gannot, E. Vincent, S. Markovich-Golan, and A. Ozerov, “A consolidated perspective on multimicrophone speech enhancement and source separation,” *IEEE/ACM Transactions on Audio, Speech, and Language Processing (TASLP)*, vol. 25, no. 4, pp. 692–730, 2017.
- [6] Y. Luo and N. Mesgarani, “Conv-TasNet: Surpassing ideal time–frequency magnitude masking for speech separation,” *IEEE/ACM Transactions on Audio, Speech, and Language Processing (TASLP)*, vol. 27, no. 8, pp. 1256–1266, 2019.
- [7] D. S. Williamson, Y. Wang, and D. Wang, “Complex ratio masking for monaural speech separation,” *IEEE/ACM Transactions on Audio, Speech, and Language Processing (TASLP)*, vol. 24, no. 3, pp. 483–492, 2015.
- [8] K. Tan and D. Wang, “Learning complex spectral mapping with gated convolutional recurrent networks for monaural speech enhancement,” *IEEE/ACM Transactions on Audio, Speech, and Language Processing (TASLP)*, vol. 28, pp. 380–390, 2019.
- [9] Z.-Q. Wang, P. Wang, and D. Wang, “Complex spectral mapping for single-and multi-channel speech enhancement and robust asr,” *IEEE/ACM Transactions on Audio, Speech, and Language Processing (TASLP)*, vol. 28, pp. 1778–1787, 2020.
- [10] Z. Zhang, Y. Xu, M. Yu, S.-X. Zhang, L. Chen, and D. Yu, “ADL-MVDR: All deep learning MVDR beamformer for target speech separation,” in *Acoustics, Speech and Signal Processing (ICASSP), 2021 IEEE International Conference on*. IEEE, 2021, pp. 6089–6093.
- [11] Y.-S. Lee, C.-Y. Wang, S.-F. Wang, J.-C. Wang, and C.-H. Wu, “Fully complex deep neural network for phase-incorporating monaural source separation,” in *Acoustics, Speech and Signal Processing (ICASSP), 2017 IEEE International Conference on*. IEEE, 2017, pp. 281–285.
- [12] H.-S. Choi, J.-H. Kim, J. Huh, A. Kim, J.-W. Ha, and K. Lee, “Phase-aware speech enhancement with deep complex U-net,” in *International Conference on Learning Representations*, 2018.
- [13] Y. Hu, Y. Liu, S. Lv, M. Xing, S. Zhang, Y. Fu, J. Wu, B. Zhang, and L. Xie, “DCCRN: Deep complex convolution recurrent network for phase-aware speech enhancement,” *Proc. Interspeech*, pp. 2472–2476, 2020.
- [14] Z.-Q. Wang, H. Erdogan, S. Wisdom, K. Wilson, D. Raj, S. Watanabe, Z. Chen, and J. R. Hershey, “Sequential multi-frame neural beamforming for speech separation and enhancement,” in *2021 IEEE Spoken Language Technology Workshop (SLT)*. IEEE, 2021, pp. 905–911.
- [15] H. Chen and P. Zhang, “Beam-Guided TasNet: An iterative speech separation framework with multi-channel output,” *arXiv preprint arXiv:2102.02998*, 2021.
- [16] Z.-Q. Wang, P. Wang, and D. Wang, “Multi-microphone complex spectral mapping for utterance-wise and continuous speech separation,” *IEEE/ACM Transactions on Audio, Speech, and Language Processing (TASLP)*, 2021.
- [17] Y. Luo, C. Han, and N. Mesgarani, “Empirical analysis of generalized iterative speech separation networks,” *Proc. Interspeech*, 2021.
- [18] D. Yu, M. Kolbæk, Z.-H. Tan, and J. Jensen, “Permutation invariant training of deep models for speaker-independent multi-talker speech separation,” in *Acoustics, Speech and Signal Processing (ICASSP), 2017 IEEE International Conference on*. IEEE, 2017, pp. 241–245.
- [19] V. Panayotov, G. Chen, D. Povey, and S. Khudanpur, “Librispeech: an ASR corpus based on public domain audio books,” in *Acoustics, Speech and Signal Processing (ICASSP), 2015 IEEE International Conference on*. IEEE, 2015, pp. 5206–5210.
- [20] G. Hu, “100 Nonspeech Sounds,” <http://web.cse.ohio-state.edu/pnl/corpus/HuNonspeech/HuCorpus.html>.
- [21] J. B. Allen and D. A. Berkley, “Image method for efficiently simulating small-room acoustics,” *The Journal of the Acoustical Society of America*, vol. 65, no. 4, pp. 943–950, 1979.
- [22] D. Diaz-Guerra, A. Miguel, and J. R. Beltran, “gpuRIR: A python library for room impulse response simulation with gpu acceleration,” *Multimedia Tools and Applications*, pp. 1–19, 2020.
- [23] Y. Luo, Z. Chen, N. Mesgarani, and T. Yoshioka, “End-to-end microphone permutation and number invariant multi-channel speech separation,” in *Acoustics, Speech and Signal Processing (ICASSP), 2020 IEEE International Conference on*. IEEE, 2020, pp. 6394–6398.
- [24] Y. Luo, Z. Chen, and T. Yoshioka, “Dual-path RNN: efficient long sequence modeling for time-domain single-channel speech separation,” in *Acoustics, Speech and Signal Processing (ICASSP), 2020 IEEE International Conference on*. IEEE, 2020, pp. 46–50.
- [25] D. Kingma and J. Ba, “Adam: A method for stochastic optimization,” *arXiv preprint: 1412.6980*, 2014.
- [26] E. Vincent, R. Gribonval, and C. Févotte, “Performance measurement in blind audio source separation,” *IEEE/ACM Transactions on Audio, Speech, and Language Processing (TASLP)*, vol. 14, no. 4, pp. 1462–1469, 2006.
- [27] J. Le Roux, S. Wisdom, H. Erdogan, and J. R. Hershey, “SDR – half-baked or well done?” in *Acoustics, Speech and Signal Processing (ICASSP), 2019 IEEE International Conference on*, May 2019, pp. 626–630.